Model-based wavefront reconstruction for the pyramid sensor tested on the LOOPS bench

Victoria Hutterer[a], Pierre Janin-Potiron[b,c], Iuliia Shatokhina[d], Olivier Fauvarque[b], Andreas Obereder[d], Stefan Raffetseder[d], Vincent Chambouleyron[b,c], Carlos Correia[b], Thierry Fusco[c], Benoit Neichel[b], Kacem El-Hadi[b], and Charlotte Bond[e]

[a]Industrial Mathematics Institute, Johannes Kepler University Linz, Altenbergerstrasse 69, 4040 Linz, Austria
[b]Aix Marseille Université, CNRS, CNES, LAM (Laboratoire d'Astrophysique de Marseille) UMR 7326, 13388, Marseille, France
[c]ONERA–the French Aerospace Laboratory, F-92322 Chatillon, France
[d]Johann Radon Institute for Computational and Applied Mathematics Linz, Altenbergerstrasse 69, 4040 Linz, Austria
[e]Institute for Astronomy, University of Hawaii-Manoa 640 N. Aohoku Place Hilo, HI 96720 USA

ABSTRACT

Model-based matrix-free wavefront reconstruction algorithms have proven to provide highly accurate results for both Shack-Hartmann and pyramid wavefront sensors in various simulation environments (OCTOPUS, YAO, COMPASS, OOMAO). Previously, test bench as well as on-sky tests were performed with the CuReD for the Shack-Hartmann sensor providing a convincing performance level together with highly reduced computational efforts. The P-CuReD is a method with linear complexity for wavefront reconstruction from pyramid sensor data which employs the CuReD algorithm and a data preprocessing step converting pyramid signals into Shack-Hartmann-like data. Here we present experimental results for the pyramid sensor being controlled with the P-CuReD on the LOOPS test bench of the Laboratoire d'Astrophysique de Marseille. Through the example of the P-CuReD a comparison of control using matrix-free Fourier domain based methods to standard interaction-matrix-based approaches is provided.

Keywords: pyramid wavefront sensor, wavefront reconstruction, model-based algorithms, test bench

INTRODUCTION

For many future adaptive optics (AO) systems and especially for the new generation of extremely large telescopes (ELTs) the pyramid wavefront sensor (PWFS) has become an attractive prospect by setting new standards for AO correction quality. The sensor was proposed for the first time as a promising alternative to other types of wavefront measuring devices such as the commonly used Shack-Hartmann (SH) sensor in the 90s.[1] For several of the instruments planned for future ELTs such as METIS, MICADO, HARMONI, NFIRAOS, EPICS etc.[2–5] the pyramid sensor has nowadays emerged as a prime candidate for the baseline. This is due to the high sensor sensitivity within the AO correction band combined with a reduced susceptibility to aliasing.[6]

The pyramid wavefront sensing is based on optical Fourier filtering.[7] In a focal plane, light falling onto the telescope aperture represented by the characteristic function $\mathbb{1}_P$ is focused on the top of a 4-sided pyramidal prism. Due to the splitting by the prism described by the optical transfer function OTF, the light propagates into 4 slightly different directions and is re-imaged into 4 pupil images that contain phase information Φ encoded as intensity variations. A detector captures the intensity patterns

$$I(x,y) = \left|\mathcal{F}^{-1}\left(OTF \cdot \mathcal{F}\left(\mathbb{1}_P e^{-i\Phi}\right)\right)\right|^2$$

Further author information: (Send correspondence to Victoria Hutterer)
Victoria Hutterer: E-mail: victoria.hutterer@indmath.uni-linz.ac.at, Telephone: +43 732 2468 4108

by counting the number of incident photons over a short exposure time. Afterwards, the 4 pupil images are cut out and combined as[6]

$$s_x(m,n) = \frac{(I_1 + I_3 - I_2 - I_4)(m,n)}{I_{total}}, \qquad s_y(m,n) = \frac{(I_1 + I_2 - I_3 - I_4)(m,n)}{I_{total}} \tag{1}$$

in the so-called *slopes map approach*. The intensity in the j-th pyramid pupil for $j = 1, 2, 3, 4$ is given by $I_j(m,n)$ and the average intensity contained within the valid regions of all 4 pupil images is denoted by I_{total}. In the slopes map approach, the 2 signals are close to the derivative of the wavefront in x- and y-direction (similar to a SH sensor) especially when a high modulation amplitude is applied to the PWFS. Note that it is also possible to capture the full frame image of the intensities known as *full-frame approach* and to control the AO loop on basis of these data.[8] However, the model-based algorithm we investigate in this paper is based on the slopes representation (1) of the signal.

Recently, a lot of model-based and matrix-free approaches for wavefront reconstruction from pyramid wavefront sensor data have been developed[9–19] and extensively reviewed in 20. A very promising reconstructor candidate with respect to accuracy, stability, and computational complexity is the *preprocessed cumulative reconstructor with domain decomposition* (P-CuReD).[9] Its outstanding performance has already been thoroughly tested in end-to-end simulation environments such as Octopus, YAO, or OOMAO.[21–25] Here we present an experimental validation of the reconstructor carried out at the LAM/ONERA pyramid sensor (LOOPS) optical bench[26–28] in the Laboratoire d'Astrophysique de Marseille (LAM) and include comparisons with AO simulations in OOMAO – the software which is also used to realize the real-time control on the bench.

In section 1 we describe the optical setup of the pyramid bench followed by details about the utilized model-based reconstructor given in section 2. Experimental results are then presented in section 3 as well as additional numerical simulations in section 4.

1. SETUP OF THE OPTICAL BENCH AND REAL-TIME CONTROL

The optical layout of the LOOPS bench is shown in figure 1 and figure 2. The experimental setup consists of a laser as monochromatic light source with a wavelength $\lambda = 635$ nm. The turbulent atmosphere is simulated by a rotating phase screen for which the effective turbulence is of $d/r_0 = 3.2$ where d is the actuator spacing and r_0 the Fried parameter. Corresponding to $d = 50$ cm and $r_0 = 15.5$ cm this turbulence is representative of strengths expected to be present at extremely large telescopes.[27] The system is controlled by a 9×9 ALPAO deformable mirror (DM) having $n_a = 69$ active actuators in total. The pyramid wavefront sensor focal phase mask is realized by a spatial light modulator (SLM). The pupil image is sampled with 80 pixels across the diameter, i.e. roughly a factor 10 oversampling with regards to the DM69. The four images of the pupil which are then combined according to the slopes map approach as presented in equation (1), are realized by the incorporated OCAM^2 camera. The circular beam modulation with an amplitude of about $5\lambda/D$ around the pyramid top is produced by a fast tip-tilt mirror at 500 Hz. In some of the test cases we also considered the non-modulated pyramid wavefront sensor. For the alignment and in order to obtain reference measurements additional flat mirrors are installed on the bench. As already indicated in previous works[7,27] it is important to take a reference WFS measurement corresponding to a flat wavefront such that the closed AO loop remains stable around the zero phase.

The AO real-time control is realized using OOMAO.[25] This makes it straightforward for additional numerical tests of various algorithms. These are performed in section 4. Note that comparisons between experiments on this pyramid bench and simulations have already been performed before[27] and verified the accuracy of the end-to-end simulation environment OOMAO. Cameralink is utilized as commutative interface between the OCAM^2 camera and a Matlab routine in order to control the DM of the AO system. The AO loop frame rate is approximately 300 Hz.

The performance assessment is estimated from a measurement of the final PSF provided by an imaging camera. Comparative wavefront measurements are also provided by a SH sensor with 32 lenslets across the pupil.

The reconstructor applied for the experimental studies discussed in this paper is the P-CuReD method described in the next section.

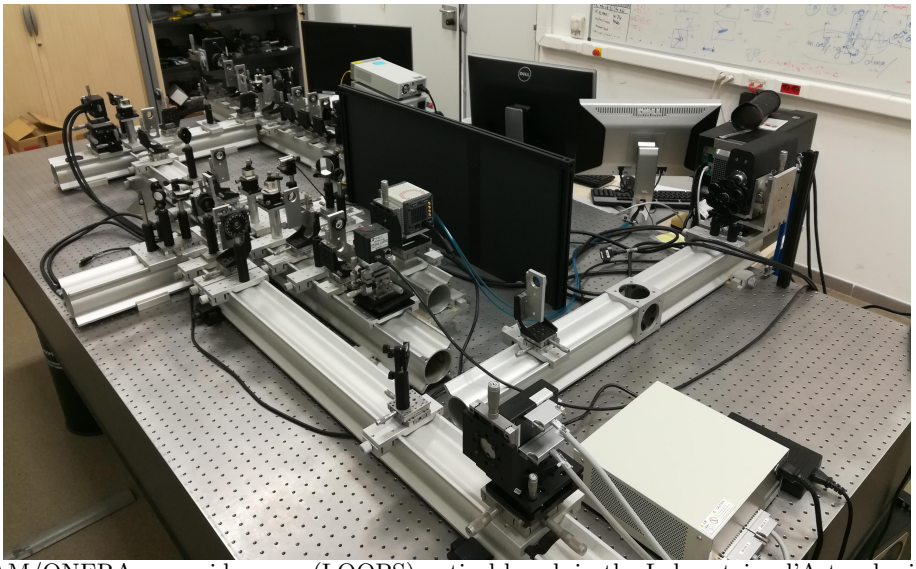

Figure 1: The LAM/ONERA pyramid sensor (LOOPS) optical bench in the Laboratoire d'Astrophysique de Marseille.

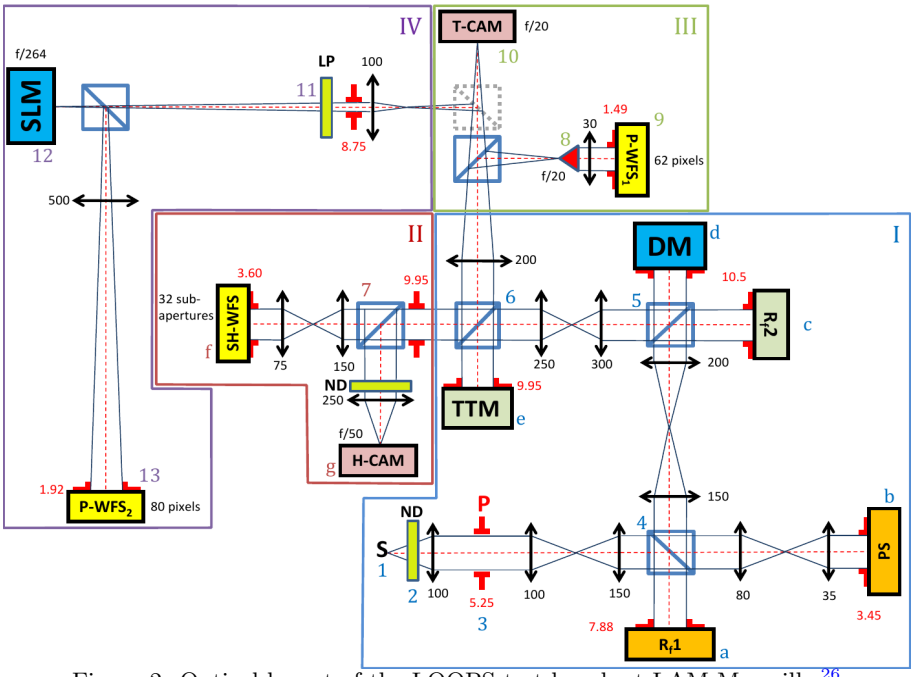

Figure 2: Optical layout of the LOOPS test bench at LAM Marseille.[26]

2. ALGORITHMIC DESCRIPTION OF THE P-CURED METHOD

The preprocessed cumulative reconstructor with domain decomposition[9] is a two step approach consisting of a data preprocessing part and the application of a reconstructor for Shack-Hartmann sensors – the CuReD.[29–32] The idea is applicable to pyramid sensors with no or any arbitrary modulation amplitude α in a linear or circular setting. A convincing feature of the P-CuReD used as wavefront reconstruction method for pyramid sensors is the low computational load of the algorithm by simultaneously providing exceptional quality performance. With a linear complexity the algorithm is, to our knowledge, the fastest reconstruction method available for pyramid sensors. Its reconstruction results match and often outperform those obtained by interaction-matrix-based approaches as later demonstrated in section 4.

2.1 Step 1: data preprocessing

The first step, the data preprocessing, is based on an analytical Fourier domain (FD) relation between linearized pyramid sensor data and Shack-Hartmann sensor data. This FD relation to SH measurements is given by

$$\mathcal{F}\left\{s_{sh}\right\}(\xi) = \mathcal{F}\left\{s_{pyr}\right\}(\xi) \cdot g_{sh/pyr}(\xi), \tag{2}$$

where the measurements s_{sh} or s_{pyr} indicate Shack-Hartmann or pyramid sensor data respectively and $g_{sh/pyr}$ the pyramid-to-SH transmission filter. The pyramid signal s_{pyr} is in this setting approximated by

$$s_{pyr}(x,y) = \frac{1}{\pi} \int_{\Omega_y} \frac{\Phi(x',y) \cdot k^{\{n,l,c\}}\left(\alpha\left(x'-x\right)\right)}{x'-x} \, \mathrm{d}x' \tag{3}$$

for

$$\begin{aligned} k^n(x) &:= 1, \\ k^l(x) &:= \operatorname{sinc}(x), \\ k^c(x) &:= \frac{1}{\pi} \int_0^{\pi} \cos\left(x \cos t\right) \, dt \end{aligned}$$

representing no modulation n, linear modulation l, and circular modulation c. Note that for simplicity of notation, we only consider measurements in x-direction here and denote them by s_{sh} or s_{pyr} respectively. However, the theory is applicable to data in both directions s_x and s_y (1). For the spatial frequency ξ we consider the interval $[-\xi_{cut}, \xi_{cut}]$ with cut-off frequency $\xi_{cut} = 1/(2d)$. The term Ω_y represents one string of the telescope aperture for fixed y. For further details on the various underlying approximate pyramid sensor models we refer the reader to 15. In the simplified setting (3) the measurements are decoupled for x- and y-direction such that all these considerations can be made in 1d. Based on (2) the pyramid-to-SH transmission filter $g_{sh/pyr}$ can be formulated as

$$g_{sh/pyr}(\xi) := \frac{\mathcal{F}\left\{s_{sh}\right\}(\xi)}{\mathcal{F}\left\{s_{pyr}\right\}(\xi)} = \frac{g_{sh}(\xi)}{g_{pyr}(\xi)},$$

where g_{sh}, g_{pyr} describe the SH or pyramid filter functions. As derived in 6,9, for the non-modulated sensor the transmission filter is represented by

$$g^n_{sh/pyr}(\xi) = 2\pi d\xi \operatorname{sgn}(\xi) \qquad \forall \xi \in [-\xi_{cut}, \xi_{cut}],$$

for the linearly modulated sensor by

$$g^l_{sh/pyr}(\xi) = \begin{cases} 2\pi d\xi \operatorname{sgn}(\xi), & |\xi| > \xi_{mod}, \\ 2\pi d\xi_{mod}, & |\xi| \leq \xi_{mod}, \end{cases}$$

and for the circularly modulated sensor by

$$g^{c}_{sh/pyr}(\xi) = \begin{cases} 2\pi d\xi \,\mathrm{sgn}(\xi), & |\xi| > \xi_{mod}, \\ \dfrac{\pi^2 d\xi}{\arcsin(\xi/\xi_{mod})}, & |\xi| \leq \xi_{mod}. \end{cases}$$

For a modulation amplitude α and sensing wavelength λ, the parameter $\xi_{mod} = \alpha/\lambda$ indicates the frequency at which the transition between the two regimes of the pyramid sensor (slope versus phase mode) emerges.[6] Converting the transmission filters into space domain kernels by the application of the inverse Fourier transform, i.e.,

$$p_{sh/pyr}(x) = \mathcal{F}^{-1}\left\{g_{sh/pyr}\right\}(x)$$

and choosing a suited discretization approach, we end up with a representation of the kernels having only few nonzero values as, e.g., shown in figure 3. Thus, the data preprocessing

$$s_{sh}(x) = \frac{1}{\sqrt{2\pi}}\left(s_{pyr} * p_{sh/pyr}\right)(x)$$

which is approximated as a row- and column-wise convolution of the measurements with the corresponding kernel has (as the CuReD) linear complexity, and thus is computationally cheap.

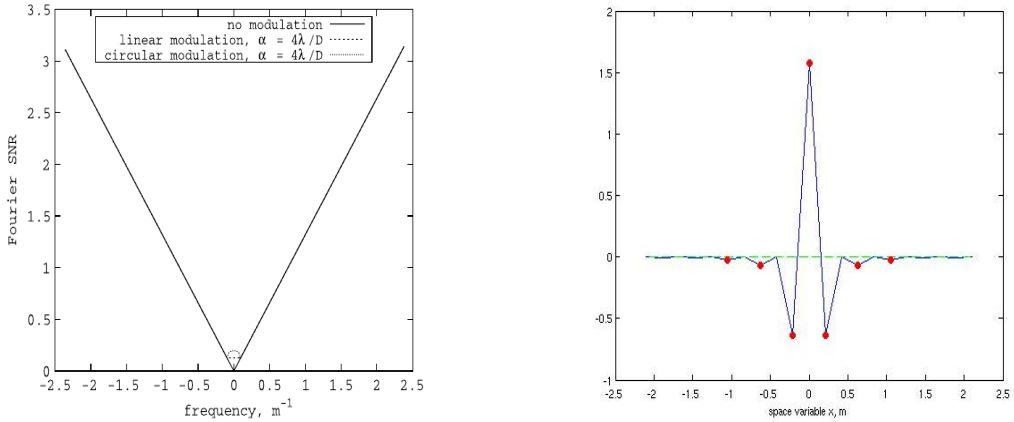

Figure 3: Pyramid-to-SH transmission filters in the Fourier domain (left) and pyramid-to-SH transmission kernel in the space domain for modulation 4 λ/D using 7 evaluation points (right). The difference induced by the modulation between the FD-filters is only in the low frequency domain.

2.2 Step 2: application of the CuReD

After the pyramid sensor measurements have been transformed into SH-like data, the CuReD[31] algorithm is applied to the modified pyramid signal. Besides detailed studies based on numerous closed loop end-to-end simulations, tests on sky proved a high-quality and high-speed performance of the CuReD for SH sensors.[33,34]

2.3 The P-CuReD

Combining both steps we obtain an accurate wavefront reconstruction method with a complexity of $\mathcal{O}(n_a)$.

An advantage of the P-CuReD is the ease of usage compared to other approaches since no optimization of intrinsic regularization parameters is needed during the reconstruction process, for instance, if atmospheric conditions change. Several AO simulation tool users performed simulations and compared the performances of diverse matrix-vector-multiplication (MVM) methods with the P-CuReD, e.g., for XAO settings utilizing the European Southern Observatory's end-to-end simulation Octopus in 35, 36. In 36 a variant of a modal

MVM approach and the P-CuReD algorithm give almost the same reconstruction quality with only very slight discrepancies. Moreover, in the latter reference a faster convergence of the P-CuReD to high Strehl ratios compared to the tested MVM approach was shown.

In principle, the data preprocessing step described in section 2.1 can be applied in combination with any other reconstructor for Shack-Hartmann wavefront sensors. The Austrian adaptive optics team reports first attempts in 37, 38 to combine data preprocessing with the *finite element-wavelet hybrid algorithm* (FEWHA)[39] – an algorithm for atmospheric tomography systems as multi-conjugate AO.

For segmented pupils the P-CuReD algorithm combined with a *direct segment piston reconstructor* (DSPR)[37,40] shows superb performance with hardly any loss in quality compared to simulations without telescope spiders realized for the METIS instrument on the ELT. This scheme is known as *split approach*.

2.4 DM fitting

The P-CuReD algorithm is a representative of decoupled methods in AO control. In this approach the wavefront reconstruction and the DM fitting equations are considered independently from each other and solved in two separate consecutive steps. The standard (coupled) approach (e.g., inversion of the calibration-based interaction matrix), on the contrary, combines the DM with the WFS and solves the coupled WFS-to-DM equation in one step.

From the experience with the decoupled approach it is known that, due to small residuals in closed loop operation, the DM fitting equation can be solved approximately, i.e., without using the actual shape of the DM influence functions. Instead, the reconstruction represented in the basis of artificial bilinear functions is projected (interpolated) onto the DM actuator positions. However, in case the WFS is oversampled with respect to the DM, a DM fitting step has to be solved. In this case, the overall complexity of the control increases by $\mathcal{O}(n_a^2)$ needed for mapping the wavefront onto the DM.

Note that the P-CuReD algorithm can also be implemented as an MVM since both steps of the algorithm are linear. In the non-oversampled case an implementation of the P-CuReD as an MVM is not desired as its main advantage, the low complexity of $\mathcal{O}(n_a)$, gets lost. In case of an oversampled DM, the DM fitting step dominates in the overall computational costs. Therefore, a formulation of P-CuReD as an MVM allows to combine the reconstruction and DM fitting step to a single MVM costing $\mathcal{O}(n_a^2)$ in total.

3. EXPERIMENTAL VALIDATION OF MODEL-BASED ALGORITHMS

Studies on the optical bench LOOPS described in section 1 were performed for a pyramid sensor without modulation and a pyramid sensor having a modulation of around $5\lambda/D$. As reconstructor we used the model-based, matrix-free algorithm P-CuReD. The shape of the incoming wavefront was estimated and afterwards projected onto the DM. The used influence functions were previously measured by the SH sensor installed on the bench.

The long exposure PSFs shown in figure 4 validate the experimental closed loop performance of the P-CuReD. The experiments have shown that the P-CuReD provides an accuracy similar to modal MVM approaches using a calibrated system matrix. Especially remarkable is the ability to control the AO loop for the non-modulated pyramid sensor using P-CuReD since the sensor without modulation suffers more from the non-linearity in that regime. Although not applied for the studies presented in this paper, the possibility of a frequency dependent control for a compensation of the optical gain of the PWFS can be realized by the preprocessing kernel used in the P-CuReD. Further details on optical gain compensation for AO control using interaction-matrix-based approaches or the P-CuReD can be found in 41,42. However, the LE PSF in figure 4 left shows that even without optical gain compensation we are able to close the loop for the non-modulated PWFS using the P-CuReD for wavefront reconstruction.

Due to technical reasons it was, unfortunately, not possible to measure any Strehl ratios on the LOOPS bench when the experiments were executed.

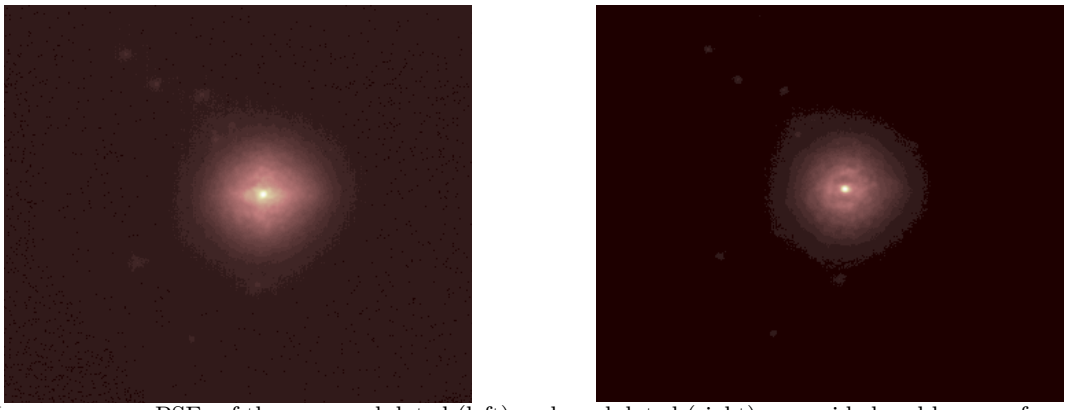

Figure 4: Long exposure PSFs of the non-modulated (left) and modulated (right) pyramid closed loop performance using P-CuReD on the LOOPS bench.

4. ADDITIONAL STUDIES USING OOMAO END-TO-END SIMULATIONS

In order to have further comparisons between interaction-matrix-based approaches and the P-CuReD algorithm in a setting similar to the LOOPS bench, we performed several OOMAO simulations for various guide star (GS) magnitudes. The tests were realized for an $80x80$ PWFS at a sensing wavelength of $\lambda = 640$ nm and modulation 5 λ/D. Turbulence strength and other simulation parameters were chosen according to those presented in section 1 for the optical bench itself. As interaction-matrix-based approach a modal MVM with a truncated singular value decomposition as regularization was applied. The corresponding long exposure Strehl ratios in R-band are presented in figure 5. Corresponding results for a PWFS without modulation and a bright star are 30.5% for P-CuReD versus 24.7% for modal MVM (without specific compensation of the optical gain of the pyramid sensor). Further simulations using the non-linear algorithm Kaczmarz-Landweber iteration for pyramid sensors (KLIPS)[17] for wavefront reconstruction provided very remarkable results. With a Strehl ratio of 31.9% for a non-modulated PWFS the KLIPS is outperforming both MVM and P-CuReD. The benefit of this method is that it estimates the wavefront and deals with the non-linearity of the PWFS at once, i.e., no further optical gain compensation is necessary.

Overall, the bench and simulation tests show that the P-CuReD accuracy is highly comparable to those of MVM and even outperforms the latter for bright GS magnitudes. These results indicate the powerful performance of the P-CuReD and match the simulation comparisons presented in 19 for a Sphere-like setting and in 42 investigating pyramid sensors for K- and R-band sensing.

CONCLUSIONS

In this paper we have presented the latest experiments achieved on the LOOPS test bench at LAM for a system applying a pyramid wavefront sensor and the P-CuReD as wavefront reconstructor. We have accomplished an experimental validation of the P-CuReD by closing the AO loop for a pyramid sensor with and without modulation.

In addition to the experiments, we have presented further numerical OOMAO simulations comparing the performance of the P-CureD to a modal MVM in a setting similar to the bench, i.e., for a PWFS sensing in the R-band. The tests verify the similar accuracy of both reconstructors with the P-CuReD outperforming the MVM with respect to the computational complexity.

The convincing results from both bench and numerical simulations show that it is highly desirable to perform extended experimental studies on model-based reconstructors in general and especially on the P-CuReD method. Furthermore, test bench investigations on pyramid sensors integrated in systems having wide telescope spider structures are interesting future work in order to show the stability of the AO control using reconstructors as the P-CuReD in the split approach[37,40] for segmented primary mirrors on ELTs.

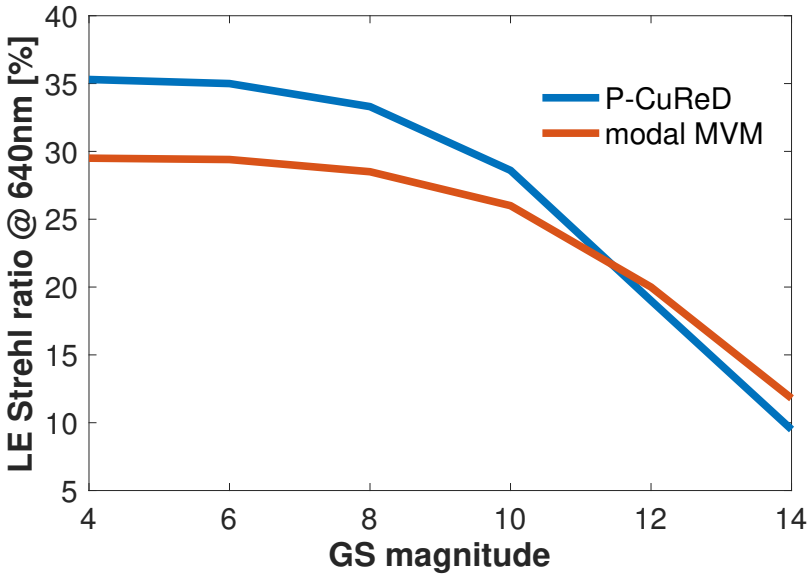

Figure 5: R-band Strehl ratio in closed loop versus guide star magnitude for a pyramid wavefront sensor with modulation using P-CuReD and a modal MVM approach.

Very promising bench simulation results were, additionally, obtained with the non-linear reconstructor KLIPS for the non-modulated pyramid sensor. The algorithm's superior performance in simulations of especially non-modulated PWFSs sensing in short wavelengths indicates that further tests of the non-linear KLIPS on the bench are particularly interesting for future investigations.

ACKNOWLEDGMENTS

The authors acknowledge the support of the Austrian Federal Ministry of Science and Research (HRSM) and the Austrian Science Fund (F68-N36, project 5). Moreover, the research leading to these results received the support of the A*MIDEX project (no. ANR-11-IDEX-0001- 02) funded by the Investissements d'Avenir French Government program, managed by the French National Research Agency (ANR).

REFERENCES

[1] Ragazzoni, R., "Pupil plane wavefront sensing with an oscillating prism," *J. of Modern Optics* **43**(2), 289–293 (1996).

[2] Brandl, B. et al., "Status of the mid-infrared E-ELT imager and spectrograph METIS," *Proc. SPIE* **9908**, 9908 – 9908 – 15 (2016).

[3] Davies, R. et al., "The MICADO first light imager for the ELT: overview, operation, simulation," in [*Proc. SPIE*], 10702 – 107021S (2018).

[4] Neichel, B., Fusco, T., Sauvage, J.-F., Correia, C., Dohlen, K., El-Hadi, K., Blanco, L., Schwartz, N., et al., "The adaptive optics modes for HARMONI: from Classical to Laser Assisted Tomographic AO," in [*Proc. SPIE 9909, Adaptive Optics Systems V*], 990909–990909–15 (2016).

[5] Kasper, M., Beuzit, J.-L., Vérinaud, C., et al., "EPICS: direct imaging of exoplanets with the E-ELT," in [*Proc. SPIE*], **7735**, 7735–7735–9 (2010).

[6] Vérinaud, C., "On the nature of the measurements provided by a pyramid wave-front sensor," *Optics Communications* **233**, 27–38 (2004).

[7] Fauvarque, O., Neichel, B., Fusco, T., Sauvage, J.-F., and Girault, O., "General formalism for Fourier-based wave front sensing: application to the pyramid wave front sensors," in [*Journal of Astronomical Telescopes, Instruments, and Systems (JATIS)*], *Proc SPIE* **3** (01 2017).

[8] Fauvarque, O., Schatz, L., Janin-Potiron, P., Chambouleyron, V., Hutterer, V., Correia, C., Sauvage, J.-F., Neichel, B., Fusco, T., and Brûlé., Y., "Full-Frame vs. Slopes-Maps: impact on the Pyramid WFS's sensitivity and linearity," in [*Poster at AO4ELT6*], (2019).

[9] Shatokhina, I., Obereder, A., Rosensteiner, M., and Ramlau, R., "Preprocessed cumulative reconstructor with domain decomposition: a fast wavefront reconstruction method for pyramid wavefront sensor," *Applied Optics* **52**(12), 2640–2652 (2013).

[10] Shatokhina, I. and Ramlau, R., "Convolution- and Fourier-transform-based reconstructors for pyramid wavefront sensor," *Applied Optics* **56**(22), 6381–6390 (2017).

[11] Shatokhina, I., *Fast Wavefront Reconstruction Algorithms for eXtreme Adaptive Optics*, PhD thesis (11 2014).

[12] Bond, C. Z., Correia, C. M., Sauvage, J.-F., Neichel, B., and Fusco, T., "Iterative wave-front reconstruction in the fourier domain," *Opt. Express* **25**, 11452–11465 (2017).

[13] Bond, C. Z., Correia, C. M., Sauvage, J.-F., Hadi, K. E., Neichel, B., and Fusco, T., "Fourier wavefront reconstruction with a pyramid wavefront sensor," in [*Proc. SPIE*], **10703**, 10703 – 107034M – 8 (2018).

[14] Hutterer, V. and Ramlau, R., "Wavefront reconstruction from non-modulated pyramid wavefront sensor data using a singular value type expansion," *Inverse Problems* **34**(3), 035002 (2018).

[15] Hutterer, V., Ramlau, R., and Shatokhina, I., "Real-time adaptive optics with pyramid wavefront sensors: part I. a theoretical analysis of the pyramid sensor model," *Inverse Problems* **35**, 045007 (03 2019).

[16] Hutterer, V., Ramlau, R., and Shatokhina, I., "Real-time adaptive optics with pyramid wavefront sensors: part II. accurate wavefront reconstruction using iterative methods," *Inverse Problems* **35**, 045008 (03 2019).

[17] Hutterer, V. and Ramlau, R., "Nonlinear wavefront reconstruction methods for pyramid sensors using Landweber and Landweber-Kaczmarz iteration," *Appl. Opt.* **57**, 8790–8804 (10 2018).

[18] Hutterer, V., *Model-based wavefront reconstruction approaches for pyramid wavefront sensors in Adaptive Optics*, PhD thesis, Johannes Kepler University Linz (2018).

[19] Correia, C. M., Fauvarque, O., Bond, C. Z., Shatokhina, I., and Hutterer, V., "Matrix-free real-time wavefront reconstruction with pyramid sensors," in [*Poster at AO4ELT6*], (2019).

[20] Shatokhina, I., Hutterer, V., and Ramlau, R., "Review on methods for wavefront reconstruction from pyramid wavefront sensor data," (2019). submitted.

[21] Le Louarn, M., Vérinaud, C., Korkiakoski, V., Hubin, N., and Marchetti, E., "Adaptive optics simulations for the european extremely large telescope," in [*SPIE Astronomical Telescopes+Instrumentation*], 627234–627234, International Society for Optics and Photonics (2006).

[22] Le Louarn, M., Vérinaud, C., Korkiakoski, V., and Fedrigo, E., "Parallel simulation tools for AO on ELTs," in [*Advancements in Adaptive Optics*], *Proc. SPIE 5490*, 705–712 (2004).

[23] Rigaut, F. and van Dam, M., "ELT AO simulations on a laptop with YAO," in [*Proc. AO4ELT3*], (2013).

[24] Rigaut, F. and Van Dam, M., "Simulating astronomical Adaptive Optics systems using yao," *Proc. AO4ELT3*, 18 (2013).

[25] Conan, R. and Correia, C., "Object-oriented matlab adaptive optics toolbox," in [*Proc. SPIE*], **9148**, 9148–9148–17 (2014).

[26] Janin-Potiron, P., Chambouleyron, V., Schatz, L., Fauvarque, O., Bond, C. Z., Abautret, Y., Muslimov, E., El-Hadi, K., Sauvage, J.-F., Dohlen, K., Neichel, B., Correia, C. M., and Fusco, T., "Adaptive optics with programmable fourier-based wavefront sensors: a spatial light modulator approach to the lam/onera on-sky pyramid sensor testbed," *Journal of Astronomical Telescopes, Instruments, and Systems* **5**(3), 1 – 10 – 10 (2019).

[27] Bond, C. Z., Correia, C. M., Sauvage, J.-F., Hadi, K. E., Abautret, Y., Neichel, B., and Fusco, T., "Optimized calibration of the adaptive optics system on the LAM Pyramid bench," in [*Proceedings AO4ELT5*], (2017).

[28] Hadi, K. E., Vignaux, M., and Fusco, T., "Development of a pyramid wave-front sensor," in [*Proceedings of the Third AO4ELT Conference*], (2013).

[29] Neubauer, A., "A new cumulative wavefront reconstructor for the Shack - Hartmann sensor," *J. Inv. Ill-Posed Problems* **21**, 451–476 (2013).

[30] Rosensteiner, M., "Cumulative reconstructor: fast wavefront reconstruction algorithm for extremely large telescopes," *J. Opt. Soc. Am. A* **28**, 2132–2138 (10 2011).

[31] Rosensteiner, M., "Wavefront reconstruction for extremely large telescopes via CuRe with domain decomposition," *J. Opt. Soc. Am. A* **29**, 2328–2336 (11 2012).

[32] Zhariy, M., Neubauer, A., Rosensteiner, M., and Ramlau, R., "Cumulative wavefront reconstructor for the Shack-Hartman sensor," *Inverse Problems and Imaging* **5**, 893–913 (11 2011).

[33] Bitenc, U., Basden, A., Bharmal, N. A., Morris, T., Dipper, N., Gendron, E., Vidal, F., Gratadour, D., Rousset, G., and Myers, R., "On-sky tests of the CuReD and HWR fast wavefront reconstruction algorithms with CANARY," *Monthly Notices of the Royal Astronomical Society* **448**(2), 1199–1205 (2015).

[34] Bitenc, U., Rosensteiner, M., Bharmal, N., Basden, A., Morris, T., Obereder, A., Dipper, N., Gendron, E., Vidal, F., Rousset, G., Gratadour, D., Martin, O., Hubert, Z., and Myers, R., "Tests of novel wavefront reconstructors on sky with CANARY," in [*Proceedings of the Third AO4ELT Conference*], (2013).

[35] Clare, R. and Le Louarn, M., "Numerical simulations of an Extreme AO system for an ELT," in [*Proc. AO4ELT2*], 1100–1107 (2011).

[36] Clare, R. M., Engler, B. E., Weddell, S., Shatokhina, I., Obereder, A., and Le Louarn, M., "Numerical evaluation of pyramid type sensors for extreme adaptive optics for the European Extremely Large Telescope," in [*Proceedings of the Fifth AO4ELT Conference*], (2017).

[37] Obereder, A., Raffetseder, R., Shatokhina, I., and Hutterer, V., "Dealing with spiders on ELTs: using a Pyramid WFS to overcome residual piston effects," in [*Proc. SPIE*], **10703**, 10703 – 107031D – 19 (2018).

[38] Raffetseder, S., Shatokhina, I., Obereder, A., and Ramlau, R., "Atmospheric tomography with pyramid wavefront sensors for spiders," in [*Poster at AO4ELT6*], (2019).

[39] Yudytskiy, M., Helin, T., and Ramlau, R., "Finite element-wavelet hybrid algorithm for atmospheric tomography," *J. Opt. Soc. Am. A* **31**, 550–560 (03 2014).

[40] Hutterer, V., Shatokhina, I., Obereder, A., and Ramlau, R., "Advanced wavefront reconstruction methods for segmented Extremely Large Telescope pupils using pyramid sensors," *J. Astron. Telesc. Instrum. Syst.* **4**(4), 049005 (2018).

[41] Deo, V., Gendron, E., Rousset, G., Vidal, F., and Buey, T., "A modal approach to optical gain compensation for the pyramid wavefront sensor," in [*Proc. SPIE*], **10703**, 10703 – 1070320 – 18 (2018).

[42] Shatokhina, I., Hutterer, V., Obereder, A., Raffetseder, S., and Ramlau, R., "Adaptive Optics with a pyramid wavefront sensor in the visible versus near-infrared," in [*Poster at AO4ELT6*], (2019).